
Article:
Kudzotsa, I, Phillips, VTJ and Dobbie, S (2018) Effects of solid aerosols on partially glaciated clouds. Quarterly Journal of the Royal Meteorological Society, 144 (717). pp. 2634-2649. ISSN 0035-9009

https://doi.org/10.1002/qj.3376

Effects of Solid Aerosols on Partially Glaciated Clouds. †

Innocent Kudzotsa*,[a] Vaughan. T. J. Phillips, [b] Steven Dobbie, [c]

[a]*Finnish Meteorological Institute, Atmospheric Research Centre of Eastern Finland, Kuopio, Finland*

[b]*Department of Physical Geography and Ecosystem Science, Sölvegatan 12, S-223 62 Lund, Sweden*

[c]*School of Earth and Environment, University of Leeds, Leeds, UK*

*Correspondence to: *ikudzotsa@science.uz.ac.zw*: Finnish Meteorological Institute, Atmospheric Research Centre of Eastern Finland, P.O. Box 1627, 70211 Kuopio, Finland

Sensitivity tests were conducted using a state-of-the-art aerosol-cloud scheme coupled to the Weather Research and Forecasting (WRF) model to investigate the key microphysical and dynamical mechanisms by which solid aerosols affect glaciated clouds. The tests involved simulations of two contrasting cases of deep convection - a tropical maritime case and a mid-latitude continental case in which solid aerosol concentrations were increased from their pre-industrial (1850) to their present-day (2010) levels. In the mid-latitude continental case, the boosting of the number concentrations of solid aerosols weakened the updrafts in deep convective clouds resulting in reduced snow and graupel production. Consequently, the cloud fraction and the cloud optical thickness increased with increasing IN, causing a negative radiative flux change at the top of the atmosphere (TOA), i.e. a cooling effect of -1.96 $\pm$ 0.29 Wm^{-2}. On the other hand, in the tropical maritime case, increased ice nuclei invigorated upper-tropospheric updrafts in both deep convective and stratiform clouds causing cloud tops to shift upwards. Snow production was also intensified resulting in reduced cloud fraction and cloud optical thickness, hence, a positive radiative flux change at the top of the atmosphere (TOA) - a warming effect of 1.02 $\pm$ 0.36 Wm^{-2} was predicted.

Key Words: Aerosol-cloud interactions; Cloud microphysics; Cloud-resolving models; Glaciated clouds; Indirect effects; Clouds.

This article has been accepted for publication and undergone full peer review but has not been through the copyediting, typesetting, pagination and proofreading process, which may lead to differences between this version and the Version of Record. Please cite this article as doi: 10.1002/qj.3376

1. Introduction

Glaciated clouds are spatially ubiquitous and have long lifetimes in the atmosphere mostly in the form of cirrus (Platt 1973) and mixed-phase or partially glaciated clouds (Verlinde et al. 2007; Shupe et al. 2008). The average seasonal coverage of cirrus is estimated to be around 50 % over the tropics (Prabhakara et al. 1993), while over 50 % of raining precipitation in the tropics is attributed to systems that feature mixed-phase clouds (Liu 2011). Cirrus clouds are usually remnants of deep convective clouds (DCC), while mixed-phase clouds are a common feature in cumulus congestus clouds (Sheffield et al. 2015) and DCCs (Storer and Van den Heever 2013; Saleeby et al. 2016). Furthermore, DCCs are the atmosphere's conduit for transporting heat and moisture from the surface to the upper troposphere in the tropics (Fan et al. 2010). It is therefore apparent that glaciated clouds/DCCs are an integral part of the Earth's radiation and hydrological budgets.

Aerosols, on the other hand, have a profound effect on our climate system (Carslaw et al. 2013) through directly affecting the amount of radiation in the Earth-atmosphere system and also through acting as cloud condensation nuclei (CCN) or ice nuclei (IN). As a result, changes in aerosol loading affect our climate directly (Charlson et al. 1992; Haywood and Boucher 2000; Rap et al. 2013) and indirectly through modifying cloud's radiative properties - an effect known as aerosol indirect effect (AIE) (Lohmann and Feichter 2005). However, it is not presently well understood how the anthropogenic changes in aerosol loading affect the microphysical and dynamical properties of clouds (**?**) and this has been reported as the greatest source of uncertainty in climate prediction Boucher and Randall (2013); Solomon et al. (2007). Given this complex interface between aerosols and clouds and their inherent importance to the Earth's climate system, it is critical to improve our understanding of the fundamental processes underpinning aerosol-cloud interactions in order to improve climate prediction.

In this study, we investigate the key mechanisms by which changes in solid aerosol loadings, commonly known as IN modify the microphysical and dynamical properties of glaciated clouds in deep convective clouds. Most studies conducted in the past have paid more attention to CCN and warm clouds or CCN and deep convective clouds (e.g., Martin et al. 1994; Cui et al. 2006) and (Tao et al. 2007; Hoeve et al. 2011; Lee et al. 2012; Costantino and Breon 2013), while the effect of solid aerosols have received little attention (Fan et al. 2010; Gettelman et al. 2012). This deficiency emanates largely from the large uncertainties associated with the measurements and knowledge of ice nucleating aerosols (Cziczo et al. 2004; DeMott et al. 2011) and our limited comprehension of mechanisms of ice nucleation (DeMott et al. 2010; Phillips et al. 2008, 2013) as opposed to cloud droplet nucleation (**?**Petters and Kreidenweis 2007; Romakkaniemi et al. 2014). Traditionally, only insoluble hydrophobic aerosols were known to nucleate ice particles (Meyers et al. 1992; Cziczo et al. 2004; DeMott et al. 2011). However, recent laboratory studies by Murray et al. (2010) have shown that some aqueous solution droplets containing solute organic compounds can become glassy (amorphous, non-crystalline solid) under very low temperatures, which can then enable them to nucleate ice particles. Therefore, according to this discovery, it is apparent that an aerosol must be solid or an amorphous solid in order to act as an IN but does not necessarily have to be insoluble.

Some previous studies that have attempted to consider IN effects such as Van den Heever et al. (2006); Carrió et al. (2007); Fan et al. (2010) have either investigated single IN species (e.g. dust in Van den Heever et al. (2006)) or have conducted their sensitivities on isolated DCC as in (Fan et al. 2010) who in fact simultaneously perturbed the CCN and IN loadings in their sensitivity tests. As a result, there is currently no consensus on the direction or magnitude of the effects of IN on glaciated clouds, commonly known as the glaciation indirect effect (Lohmann and Feichter 2005). For example, Fan et al. (2010) concluded that the glaciation effect had a very small effect on the convective strength of updrafts in isolated DCCs, this corroborated the findings of Connolly et al. (2006) on similar cloud systems. However, Ekman et al. (2007) found that higher IN concentrations resulted in an intense glaciation effect evidenced by strong updraft velocities.

Our work differs from other previous studies in that we treat more components of ice nucleating solid aerosols; these include mineral dust (Twohy et al. 2009), soot, non-biological organics and primary biological aerosol particles (Jaenicke 2005). Here, we exclusively perturb the IN concentrations in order to only isolate the salient mechanisms by which the glaciation effect influences the microphysics and dynamics of deep convective clouds, unlike in other studies (e.g., Fan et al. 2010) where both CCN and IN were simultaneously perturbed. In addition, we study multiple multi-cell cloud systems over longer durations and larger domains allowing cell-to-cell interactions and feedbacks between clouds and their environment as opposed to the isolated clouds typically studied in the past (Lohmann 2002a; Khain et al. 2005; Connolly et al. 2006; Lee et al. 2009; Fan et al. 2012). Furthermore, in the present paper, we conduct detailed sensitivity tests on several key microphysical processes that cause the glaciation AIE, unlike in most studies where the only sensitivity tested was a change in aerosol loadings and this is an important ingredient for the development of accurate parameterizations for use in general circulation models (GCM). Finally, we quantify the process-level glaciation indirect effect or the top of the atmosphere (TOA) radiative flux changes caused by the targeted microphysical process.

We use a state-of-the-art aerosol-cloud scheme that encapsulates a robust empirical parameterization for heterogeneous ice nucleation developed by Phillips et al. (2008, 2013), which treats all the four known modes of heterogeneous ice nucleation (Diehl et al. 2001, 2002; Hoppel et al. 2002; Dymarska et al. 2006). This scheme is coupled to the Weather Research and Forecasting (WRF) model (Michalakes et al. 2005) and it treats the microphysics of cloud droplets, ice, rain, snow and graupel. Two cases of deep convection were simulated in this study, the continental Cloud and LAnd-Surface Interaction Campaign (CLASIC) (Miller 2007) and the maritime Tropical Warm Pool International Cloud Experiment (TWPICE) (May et al. 2008).

The structure of this article is as follows. In the next section, the model description and validation are provided together with an explanation of different numerical experiments conducted in this study to assess and quantify the different types of indirect effects of solid aerosols. The detailed responses of clouds to solid aerosol loading are presented and analyzed in Sect. 3, while the radiative responses of the clouds are presented in Sect. 4. Finally, conclusions will be presented in the last section, Sect. 5.

2. Model Description and Methodology

The work presented here on solid ice-nucleating aerosols is built upon recent studies of the effects of solute aerosols presented in Kudzotsa et al. (2016b,a). The cloud system resolving model (CSRM) used here is the Weather Research and Forecasting (WRF) model Version 3.6 with a unique aerosols and cloud microphysics scheme coupled to it and its full validation was presented in our previous paper (Kudzotsa et al. 2016a). Part of the methodology and some sensitivity tests used here to assess the solid aerosol indirect effects are similar to those used in another paper by Kudzotsa et al. (2016b), therefore in this section, we provide a brief description of the model and methodology to allow a smooth flow of the ideas, however the reader is refereed to those two earlier papers for a detailed description of the model, model validation and sensitivity tests.

2.1. Overview and Configuration

The aerosol-cloud microphysics scheme (Phillips et al. 2007, 2009; Kudzotsa 2013; Kudzotsa et al. 2016b) is a bin-emulating bulk scheme with two-moment prognosis of sulphate aerosols, cloud ice and cloud droplets, while a single moment approach for rain, snow and graupel is implemented in order to reduce computational power and time. Morrison et al. (2009) compared a one- and a two-moment bulk microphysics schemes in the general framework of the WRF model. This comparison was performed for a two-dimensional squall line case and it was concluded that; although, there was reduced precipitation evaporation, which led to increased rain rate and surface precipitation in the two moment scheme, the overall morphology of the of the storm feature was similar between the two models. Although, such discrepancies may arise from our quasi one-moment assumption for the precipitating species, we however, treat these species and their related processes using a bin-emulating approach, which should then compensate for the drawbacks and reduce the uncertainties associated with the one-moment representation.

The CSRM encapsulates an interactive radiation scheme from the geophysical fluid dynamics laboratory (GFDL) (Freidenreich and Ramaswamy 1999). Turbulence in the model is treated using the Medium Range Forecast (MRF) model Planetary Boundary Layer (PBL) scheme (**?**). This scheme resolves the vertical sub-grid scale fluxes caused by eddy transports and also treats horizontal and vertical mixing of fluxes provided by the surface layer and the land surface schemes. The simple soil thermal diffusion (STD) scheme is used as the land-use model. The model has non-hydrostatic and non-elastic fluid flow with periodic boundary conditions. Because the cases we simulated here were of deep convection, the model top was set at 20 km altitude and the horizontal domain was 170 km. The vertical and horizontal grid spacing were 500 m and 2 km, respectively. This spatial grid spacing is ideal in terms of computational expense and accuracy for a CSRM that covers such a large spatial domain and long duration simulations. The reliability and justification for this model grid spacing is provided in the model validation section (Subsect. 2.3). The integration time step was set at 10 seconds with prognostic variables being written out every five minutes for analysis. Convection in the model is triggered by the random perturbation at the beginning of the simulation to the moisture field and maintained by tendencies of heat and moisture that are derived from large-scale forcing observed from a network of three hourly soundings from the cases studied (May et al. 2008). However, the random perturbation that initiates the convection has a negligible impact on the model outputs due to the fact that they are driven by large scale forcing. A two-dimensional configuration was chosen for this study in order to minimize computational expense since according to Tompkins (2000) and **?**, two dimensional simulations are able to capture the key features of convective systems.

2.2. *Microphysics*

The aerosol scheme is interactive and comprises of a complement of seven different aerosol types. The aerosol types are classified into two main categories - the soluble and the solid aerosol groups. The soluble aerosol group includes ammonium sulphate, sea-salt and soluble organics, while the solid aerosol group comprises of dust, black carbon and insoluble organics. All the aerosol as listed in Table 1, which shows the lognormal distribution parameters assumed for the aerosol speicies. A γ-distribution is assumed for cloud droplets and cloud ice in the model, while other hydrometeor categories are described using an exponential distribution.

The microphysics scheme predicts the supersaturation and diffusional growth of all the five categories of hydro-meteors being treated in the model using a linearized supersaturation scheme of Phillips et al. (2007). All the aerosol types included in this model can initiate cloud droplets, while only solid aerosols can nucleate ice crystals. The primary activation of cloud droplets by soluble aerosols takes place at the cloud base using the Ming et al. (2006) scheme, while in-cloud activation is predicted using the κ-Kohler theory of Petters and Kreidenweis (2007). As for the nucleation of cloud droplets by solid aerosols, the same scheme of Petters and Kreidenweis (2007) is used for both cloud base and in-cloud droplet nucleation.

With regard to ice nucleation, the aerosol-cloud model encapsulates a robust empirical parameterization scheme for heterogeneous ice nucleation developed by Phillips et al. (2008, 2013), which treats all the four known modes of heterogeneous ice nucleation (deposition, condensation, immersion and contact freezing) (Diehl et al. 2001, 2002; Hoppel et al. 2002; Dymarska et al. 2006). The instant freezing of cloud droplets near -40 °C and the ice multiplication by the Hallet-Mossop process are some of the secondary sources of cloud ice currently being treated in the model. The ascent-dependent fraction of droplets that evaporate without freezing near -36 to -37 °C is resolved using a lookup table created by Phillips et al. (2007). This preferential evaporation of smaller droplets during homogeneous freezing is triggered by larger droplets that freeze first and cause subsaturation and was first modeled by Phillips et al. (2007) who found it causing about an order-of-magnitude impact on domain-wide average ice concentrations in systems of deep convection.

For the initiation of other hydrometeor species; the autoconversion of cloud droplets to rain is predicted according to Khairoutdinov and Kogan (2000), while the conversion from ice to snow is parameterized following the modified version of Ferrier (1994). The production of graupel from snow is riming dependent and is predicted using Swann (1998). The growth of

Aerosol group	Number of Modes	$\log_{10}$ of Standard deviation $\log_{10}(\sigma_x)$	Geometric mean, Rm_x (μm)	Solubility parameter
Sulphate (SO4)	2	0.30, 0.27; 0.049, 0.161	0.04, 0.08; 0.03, 0.18	-
Sea-Salt (SS)	2;3	0.30, 0.33; 0.05, 0.16, 0.26	0.01, 0.50; 0.03, 0.18, 4.4	-
Soluble Organics (SO)	2	0.30, 0.27; 0.049, 0.161	0.04, 0.08; 0.03, 0.18	-
Dust/Metallic (DM)	2	0.28, 0.20	0.8, 3.0	0.15
Black Carbon (BC)	1	0.20	0.2	0.80
Insoluble Organics (O)	1	0.20	0.2	0.80
Biological Aerosols (BIO)	2	0.40, 0.60	0.17, 0.47	0.80

Table 1. *Aerosol properties; the comma separates the modes, where different aerosol specifications were applied for mid-latitude continental and tropical maritime cases, a semicolon is used with the former representing CLASIC and the latter representing TWPICE.*

particles by coagulation, riming, aggregation and sedimentation are resolved by explicit integration of the continuous collection equation. This is done by creating temporary grids with 33 bins in this case upon which the respective bulk concentrations of the interacting species are decomposed according to their assumed statical distributions. After the treatment of the targeted process is completed in this bin-emulating approach, the new bulk concentrations of the species are reassembled by summing up the discretized concentrations in each bin. The full details are given in Kudzotsa (2013). This bin-emulating approach allows a bulk microphysics model to represent microphysics processes more realistically without much computational expense associated with full sectional microphysics models (Saleeby et al. 2016).

2.3. *Cases Simulated and Model Validation*

Two campaigns of relatively deep convection were chosen for this study: one is a tropical maritime case and the other is a mid-latitude continental case. In addition to their different geographical locations, the cases had very different aerosol loadings and chemistry. They provide an ideal platform for assessing the effects of solid aerosols on clouds since they exhibited typical convection that could occur over any land and any ocean and they represent the general response over these two different surface conditions and latitudes.

The first case was the Cloud and LAnd-Surface Interaction Campaign (CLASIC) (Miller 2007), which was a 3 week long continental case of deep convection. It was carried out from the 10^{th} to the 30^{th} of June in 2007 over the research facility of the U.S Department of Energy (DOE) called the Atmospheric Radiation Measurement-Climate Research Facility - Southern Great Plains (ARM-SGP) located in central U.S (lat = 36.61° and lon = 97.49°). The second case was the Tropical Warm Pool International Cloud Experiment (TWPICE) of May et al. (2008), which was a 3.5 week-long maritime case of deep convection. The TWPICE campaign stretched from the 17^{th} of January to the 12^{th} of February in 2006 over Darwin, north-west Australia (lat = -12.425° and lon = 130.891°). In addition to the references given above about these campaigns, a more detailed description was also given in Kudzotsa (2013); Kudzotsa et al. (2016a). The large scale forcing and other related data for both TWPICE and CLASIC are freely available to the public and are downloadable from the Atmospheric Radiation Measurement (ARM) Program website (`https://www.arm.gov`).

In order to contrast the thermodynamic environments of the simulated cases, Fig. 1 shows the mixed-phase depths for both the TWPICE and the CLASIC cases. The mixed-phase depth is defined by the altitudes corresponding to the homogeneous freezing level isotherm (-40 °C) and the °C isotherm. Although the mixed-phase depth of approximately 6 Km is roughly equal between the two cases, TWPICE is seen to have higher 0 °C and -40 °C than the CLASIC case. In addition, the TWIPICE case maintained a somewhat constant altitude for the two isothermal levels throughout the simulation period, whereas, for the CLASIC case, the altitudes for the isotherms were fluctuating with time. These tow thermodynamic environments cannot be directly contrasted mainly because of their different latitudinal and geographical locations in addition to the different seasons and years the campaigns were conducted. Although the two campaigns were both summer campaigns, it is expected for TWPICE to have a deeper higher freezing and homogeneous freezing level because in addition to being closer to the equator than CLASIC, February is characterized by warmest sea surface temperatures (SSTs) in

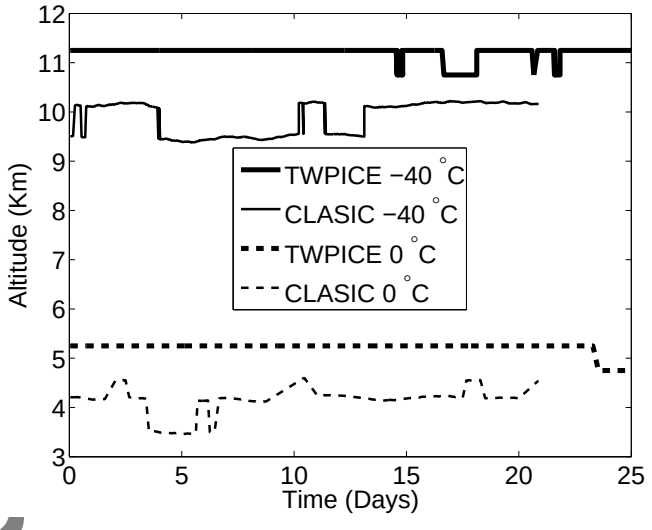

Figure 1. The time-height plot for the domain averaged mixed-phase depth (i.e the homogeneous freezing level (-40 deg C isotherms) and the freezing levels (0 deg isotherms)) of both TWPICE and CLASIC.

the southern hemisphere, which normally triggers the southern hemisphere cyclone season.

The simulations of both cases (TWPICE, CLASIC) were initialized with coincident observations of aerosol composition, size and number concentrations in addition to the standard thermodynamic soundings. The large scale forcings of temperature, pressure, wind and moisture derived from the three hourly soundings taken during the campaigns were used to force the model. The CLASIC and TWPICE cases were run for 3 and 3.5 weeks, respectively. In the model validation, the predicted droplet and ice number concentrations were compared with in-situ coincident aircraft measurements (Miller 2007; Allen et al. 2008; May et al. 2008) and they fell satisfactorily within one standard deviation from observed average values as shown in Kudzotsa et al. (2016b).

The vertical grid spacing used in this study (see Sect. 2.1) is at least an order of magnitude finer than the depth of the deep convection that was simulated. Exactly the same spatial grid spacing of the aerosol-cloud model was used in the past by Phillips et al. (2007, 2009), who comprehensively validated the 2-dimensional simulations of several cases of deep convection against aircraft, satellite and ground-based measurements for quantities including vertical velocity histograms, cloud-droplet concentrations, ice concentrations, cloud cover and surface precipitation. Also, the peak supersaturation close to cloud-base (typically about 10 meters above it) is parameterized with a dedicated cloud-base droplet activation (Nenes et al. 2006) and is not resolved, so there is no need for a fine vertical grid spacing to represent it. Our recent paper (Phillips et al. 2017) also validated a simulation of a mesoscale convective line over the US High Plains against observations of many quantities such as those mentioned above and the agreement was just as good with our 0.5 km vertical grid spacing of aerosol-cloud model as with Hebrew University Cloud Model (HUCM) (Khain et al. 2001) that uses a finer vertical grid spacing of 0.2 km.

2.4. *Methodology for Analysis of Solid Aerosol Indirect Effects*

As mentioned above in Sect. 2.2, the aerosol-cloud model comprises seven aerosol types, some of which are soluble and some being insoluble, all of which are able to activate cloud droplets. Only solid aerosols can act as ice nuclei (IN) to initiate cloud ice.

Therefore, in order to isolate the effect of solid aerosols on clouds, a couple of sensitivity tests were performed in which only the number and mass concentrations of solid aerosols were altered by changing their present-day values to their pre-industrial estimates using the percentage changes given in Table 2. These percentage changes were adapted from a modeling study of the global aerosol distributions performed by Takemura (2012). The simulation with present-day (i.e. 2010) aerosol concentration was designated as the control run and is denoted PD-CTRL, while the simulation in which the solid aerosol burden was altered to pre-industrial levels (i.e. 1850) was designated as pre-industrial simulation and is denoted PRE-IND. Both the present and the pre-industrial simulations were initialized and forced using the present-day soundings and large-scale meteorological forcing. Three key sensitivity tests were used here to isolate solid aerosol indirects on all clouds and on targeted cloud phases. Before the sensitivity tests were conducted, two identical CLASIC simulations were performed to show that differences in the model outputs due to random perturbations of the moisture field or any other processes were negligible. Below, a brief description of these tests is provided and the reader is referred to Kudzotsa (2013) and Kudzotsa et al. (2016a) for the full description of the sensitivity tests.

Solid Aerosol material	Percentage Increase (%)
Dust/Metallic (DM)	89
Black carbon (Soot) (BC)	28
Non-Biological Organic (O)	67
Biological Aerosol (BIO)	67

Table 2. Fractional changes of solid aerosol scenarios from pre-industrial (1850) to present-day (2000) for number and mass distributions (inferred from a global modelling study of the distribution of aerosols aerosol from pre-industrial to present-day scenarios Takemura (2012)).

2.4.1. *Test A: The Total Aerosol Indirect Effects*

Test A was designed to estimate the *effective total indirect effect*, F_{eff} due to solid aerosols by differencing the top of the atmosphere (TOA) radiative fluxes of the PD-CTRL and the PRE-IND simulations (i.e. $TOA_{PD-CTRL}$ - $TOA_{PRE-IND}$). This effective total indirect effect is assumed to be a simple arithmetic summation of the albedo and the lifetime indirect effects. Although, there may exist some feedbacks and compensatory responses between the lifetime and albedo indirect effects Lohmann and Feichter (2005), this assumption provides a general indication of the magnitudes and directions of the responses.

2.4.2. *Test B: Albedo and Lifetime Aerosol Indirect Effects*

The *albedo-emissivity* was estimated from this test by using two calls to the radiation scheme in both the PD-CTRL and the PRE-IND simulations. The difference between the two calls is that in the first call, the radiation scheme is allowed to fully couple with clouds by directly using droplet information being predicted in the simulation to calculate the radiative fluxes of clouds. These TOA radiative fluxes can be denoted, $TOA1_{PDCTRL}$ and $TOA1_{PRE-IND}$, respectively. In the second call to the radiation scheme, which is for diagnostic purposes only, the radiation scheme uses information on droplet sizes provided by lookup tables and is non-interacting with the cloud microphysics. These TOA radiative fluxes can be denoted, $TOA2_{PDCTRL}$ and $TOA2_{PRE-IND}$, respectively. The cloud droplet sizes in the look-up tables are temperature and vertical velocity dependent and were created offline using the present-day control simulation.

Subtracting the top of the atmosphere (TOA) radiative fluxes calculated from the first calls of the radiation scheme (i.e. $TOA1_{PDCTRL}$ - $TOA1_{PRE-IND}$), gives the effective total aerosol indirect effect, equal to F_{eff} obtained in Test A. On the other hand, differencing the top of the atmosphere (TOA) radiative fluxes calculated from the second calls of the radiation scheme (i.e $TOA2_{PDCTRL}$ - $TOA2_{PRE-IND}$), gives a hypothetical aerosol indirect effect, F_{hyp}, which is equal to F_{eff} but without cloud sizes responding to aerosol changes. By subtracting F_{hyp} from F_{eff}, the cloud albedo-emissivity effect, F_{albedo} is obtained. As explained in Test A, F_{eff} is assumed to be an arithmetic summation of the albedo and the lifetime indirect effects, the *lifetime indirect effect*, $F_{lifetime}$ is finally estimated from the difference between F_{eff} and F_{albedo} .

This technique can be applied to any targeted cloud type in order to estimate their respective contributions to the albedo or lifetime indirect effects. For instance, if the droplet or crystal sizes are selectively fixed only in mixed-phase or ice-only clouds then the albedo-emissivity and the lifetime indirect effects of mixed-phase or ice-only clouds can be respectively estimated.

2.4.3. *Test C: Isolating Lifetime Indirect Effects for Glaciated Clouds*

Test C was designed to separate the aerosol indirect effects of different cloud types such as water-only, mixed-phase or ice-only clouds. This can be achieved by fixing either the number concentrations or the sizes of cloud particles in a targeted cloud type, e.g. in liquid-only or in ice-only clouds. The fixing was done by using look-up tables of those cloud sizes in all microphysical processes dependent on cloud sizes in order to eliminate their sensitivity to aerosol changes. These vertical velocity and temperature dependent look-up tables were the same look-tables used in Test B.

Therefore, in order to isolate the lifetime indirect effects of water-only clouds, look-up tables are used in the auto-conversion, collision-coalescence, sedimentation and the radiation processes only for water-only clouds in both PD-CTRL and PRE-IND runs. By differencing the TOA radiative fluxes from the present-day and pre-industrial simulations, a hypothetical total indirect effect without the lifetime indirect effect of water-only clouds will be estimated. From this test, the lifetime indirect effect of water-only clouds is estimated and by subtracting this hypothetical indirect effect from the lifetime indirect effect derived from Test B. Finally, the glaciated cloud lifetime indirect effect is obtained by subtracting the water-only lifetime indirect effect from the total

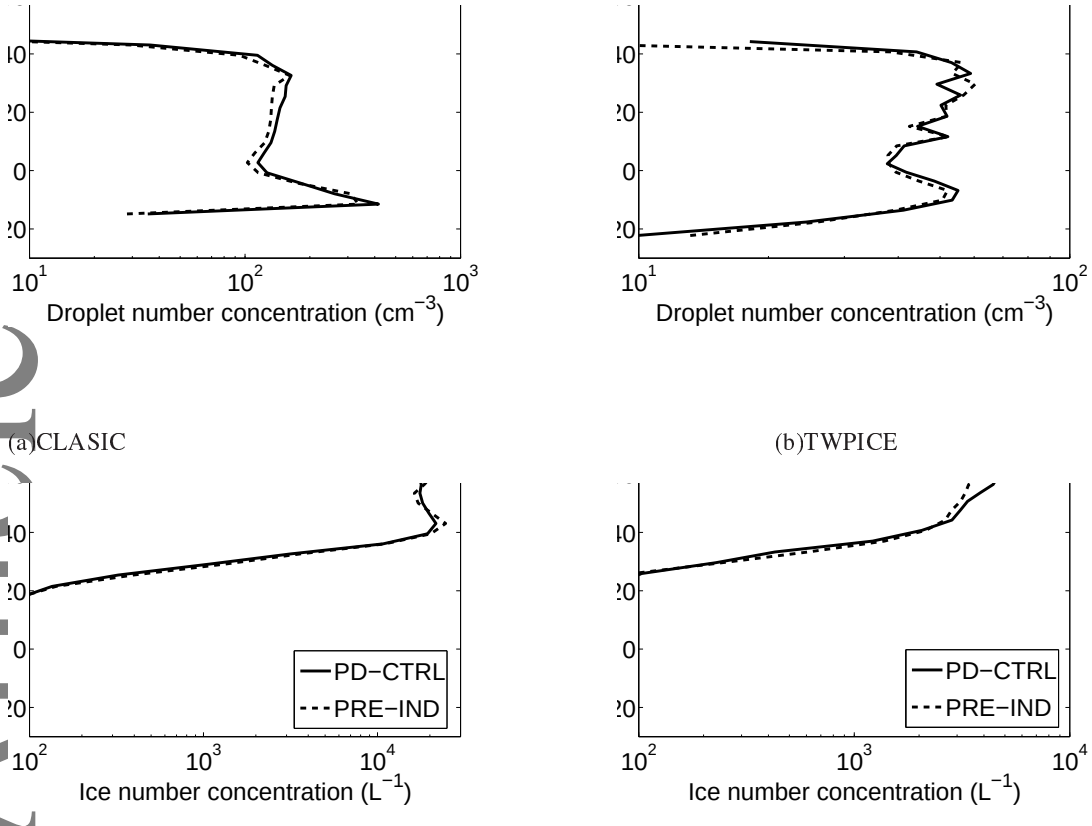

(a)CLASIC (b)TWPICE

(c)CLASIC (d) TWPICE

Figure 2. The vertical profiles of spatial and temporary averages of (a and b) cloud droplet number concentrations, (c and d) ice crystal number concentrations in deep convective clouds. The panel on the left is for the continental case, CLASIC, while the panel on the right is for the maritime case, TWPICE.

lifetime indirect effect, $F_{lifetime}$ obtained in Test B. Again, the reader is referred to Kudzotsa (2013) and Kudzotsa et al. (2016a) for further reading on these tests.

3. Results for Response of Microphysical and Dynamical Properties to Increased Solid Aerosols

In order to examine how the simulated clouds respond to changes in solid aerosol loadings, a number of microphysical and dynamical quantities representative of cloud characteristics are presented in this section for the cases simulated. Some of these quantities are plotted as spatial and temporal bulk averages representing the whole system of simulated clouds, while the other quantities are plotted as intrinsic averages. Intrinsic averages are evaluated by conditional averaging depending on the quantity being analysed, whether it is over cloudy regions, in which case, the condition would be cloud mixing ratios greater than 0.001 gkg^{-1} or over deep convective or stratiform clouds, in which case a threshold of updraft speeds greater than 1 ms^{-1} or less than 1 ms^{-1} is applied. The threshold updraft speeds of deep convective clouds is equal to what was previously used by other researchers, for example by Sheffield et al. (2015), although it was much slower than what was predicted by Saleeby et al. (2016) and Fan et al. (2010), who applied updraft speeds of greater than 3 and 7 ms^{-1}, respectively. This is because they respectively simulated isolated DCCs and a single life cycle mesoscale convective system. Most of the plots feature two curves, the solid curve representing the PD-CTRL simulation while the dashed curve represents the PRE-IND simulation.

3.1. Cloud Droplets

Droplet properties such as the number concentration and the mean size are important for both the microphysics and the dynamics of clouds and they also dictate the radiative characteristics of clouds both in the short and longwave radiation bands (Twomey 1974, 1977). Figs. 2a and 2b, show the intrinsic mean number concentration of cloud droplets averaged over deep convective clouds for CLASIC and TWPICE, respectively. The maximum peak in droplet concentration seen close to the

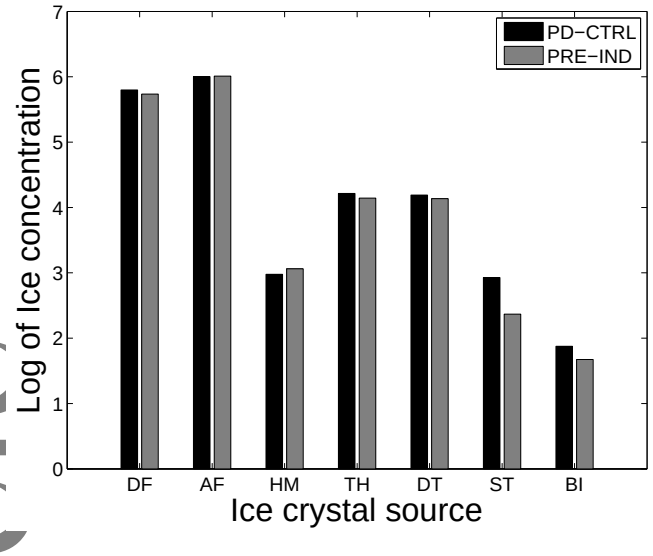

Figure 3. The ice number budget from the simulation of CLASIC, DF = droplets frozen homogeneously, AF = aerosols frozen homogeneously, HM = H-M splinters, TH = total ice from heterogeneous nucleation, (DT, ST, BI) ice from heterogeneous nucleation of dust, soot and biological organics respectively.

cloud base, particularly in CLASIC corresponds to the maximum supersaturations characteristic of cloud bases (Rogers and Yau 1991) and the behavior above the cloud bases depends on other processes such as in-cloud droplet activation and precipitation formation or growth.

The cloud droplet concentration was marginally insensitive to IN increases in both cases, although a weak bias towards an increase in present-day droplet concentration was noted in sub-zero temperatures for the CLASIC case. This insensitivity was attributed primarily to the fact that the fractional contribution of anthropogenic solid aerosol to the total present-day aerosol loading was relatively small in both cases. Secondly, although solid aerosols are able to activate cloud droplets in the model owing to their internal mixing with soluble components, their CCN activity is still relatively low in comparison to that of solute aerosols. Consequently, the droplet sizes remained largely unchanged in both cases, although a slight reduction in the mean droplet sizes of about 1 μm (plots not shown) was predicted at the corresponding heights where the increase in droplet numbers was predicted in CLASIC.

3.2. Cloud Ice

One of the hypotheses that we evaluated in this experiment was whether solid aerosols reduce the overall number of ice particles aloft by suppressing the homogeneous freezing of cloud droplets. This is expected to occur because of the glaciation indirect effect, a process by which extra solid aerosol material nucleates more ice phase that enhance ice-phase precipitation via the ice crystal process, accreting more cloud-droplets so that fewer droplets freeze homogeneously as was found in Connolly et al. (2006). However, Fan et al. (2010) found this to be strongly depended on humidity levels, especially in polluted clouds; at higher humidities the effect was more pronounced.

Although this was not distinctly pronounced, there was however a very weak evidence of this occurring in CLASIC (Fig. 2c), where a slight reduction in ice number concentrations, N_i at the very top of the cloud was predicted. Contrary to the marginally insensitive ice in CLASIC, there was a marked increase in ice concentrations above the homogeneous freezing level in the maritime case (Fig. 2d). In addition, a striking feature is shown Fig. 4d where the upward shift of cloud tops is shown in the present-day. This is attributed to the corresponding strengthening of updrafts in the upper troposphere (Figs. 5d and 5e). Although Fan et al. (2010) did not directly comment on the response of cloud-top heights to more IN, they reported an increase is upper tropospheric water vapour, which we attribute to this upward shift in cloud top height predicted in this same maritime case that they also simulated, although for an isolated DCC. Ekman et al. (2007) also showed a similar response with increase in IN loading. As for the mean sizes, there were no significant changes to the mean sizes of ice in CLASIC, although in TWPICE, there was a corresponding substantial reduction in upper tropospheric ice sizes.

Fig. 3 presents the spatial and temporal averages of ice sources in the CLASIC case, the ice number budget shows homogeneous droplet and solute aerosol freezing dominating other ice sources. This explains why there is a peak in N_i above the -40 °C altitude - the homogeneous freezing level. This is also consistent with the findings of Ekman et al. (2007) for an isolated mid-latitude continental cumulonimbus cloud. As for the Hallet-Mossop splinters, a slight reduction in H-M splinters is shown in the present-day. While there was generally a monotonic increase in heterogeneous ice nucleation resulting from increased IN, the concentrations of heterogeneously nucleated ice are about two orders of magnitude lower than those from homogeneous freezing,

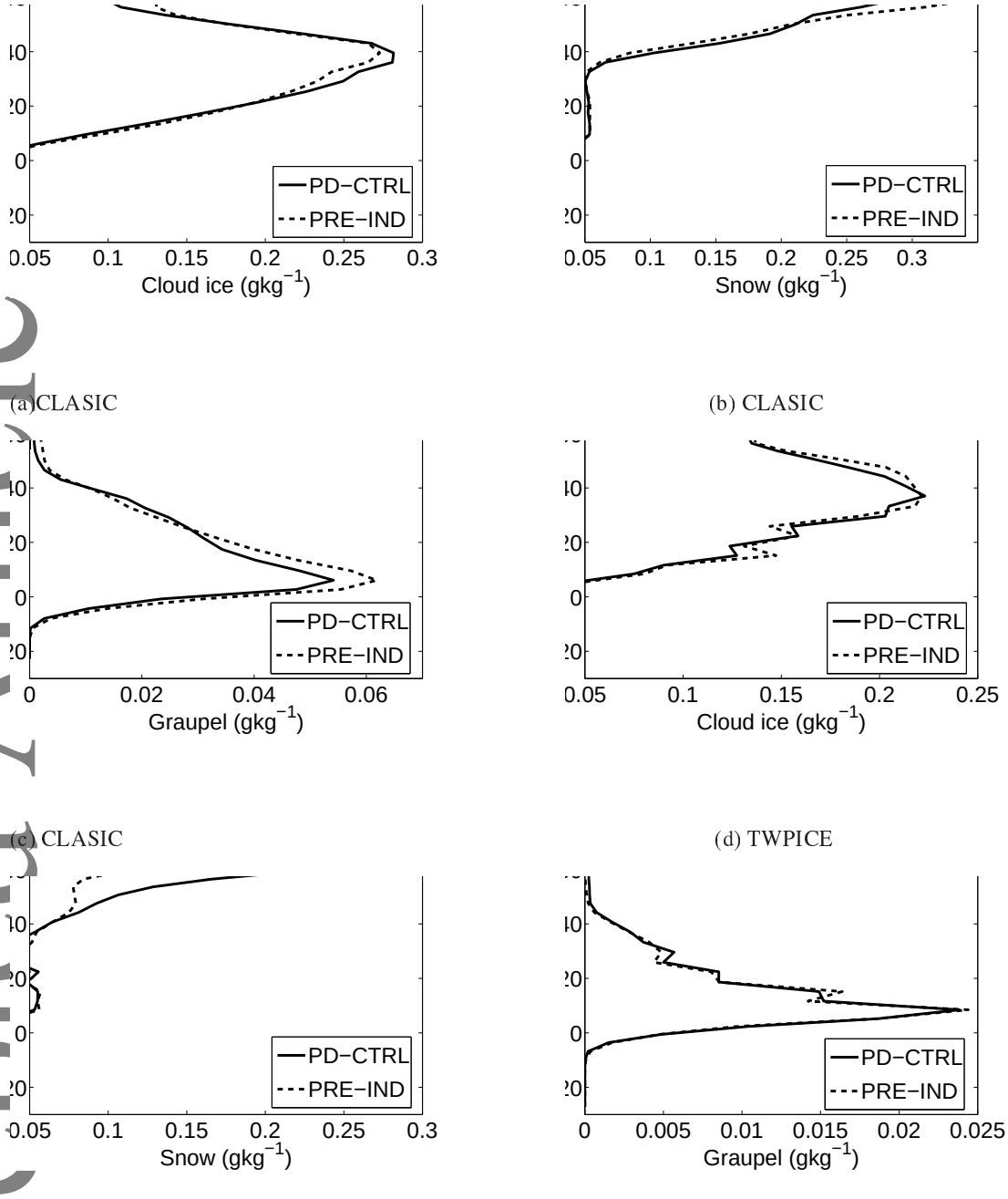

(a) CLASIC (b) CLASIC

(c) CLASIC (d) TWPICE

(e) TWPICE (f) TWPICE

Figure 4. Intrinsic spatial and temporal averages of (a) ice (b) snow and (c) graupel mixing ratios conditionally averaged over deep convective clouds. The upper panel is for the CLASIC case while the lower panel is for the TWPICE case.

as a result, the changes in ice concentrations are small. The ice number budget for the maritime cases exhibited similar features.

3.3. Water Contents and Precipitation Production

Fig. 4a shows the profiles of intrinsic ice water mixing ratios averaged over deep convective clouds in CLASIC. A peak in the profile of ice mixing ratios reminiscent of homogeneous droplet and aerosol freezing is evident close to the -40 °C level in both the PD-CTRL and PRE-IND simulations, while the second minor peak at near the -60 °C level, which is more prominent in the PRE-IND simulation is characteristic of cumulonimbus anvils. A weak trend reversal in the manner in which ice water content (IWC) responded to IN loading is exhibited in the CLASIC case; a significant loss of ice with IN loading is predicted aloft, while a significant increase of IWC is predicted below the homogeneous freezing level. The important conclusion to derive from this figure is that increased IN in this continental case actually diminishes anvil ice content. This was followed by a monotonic decrease in

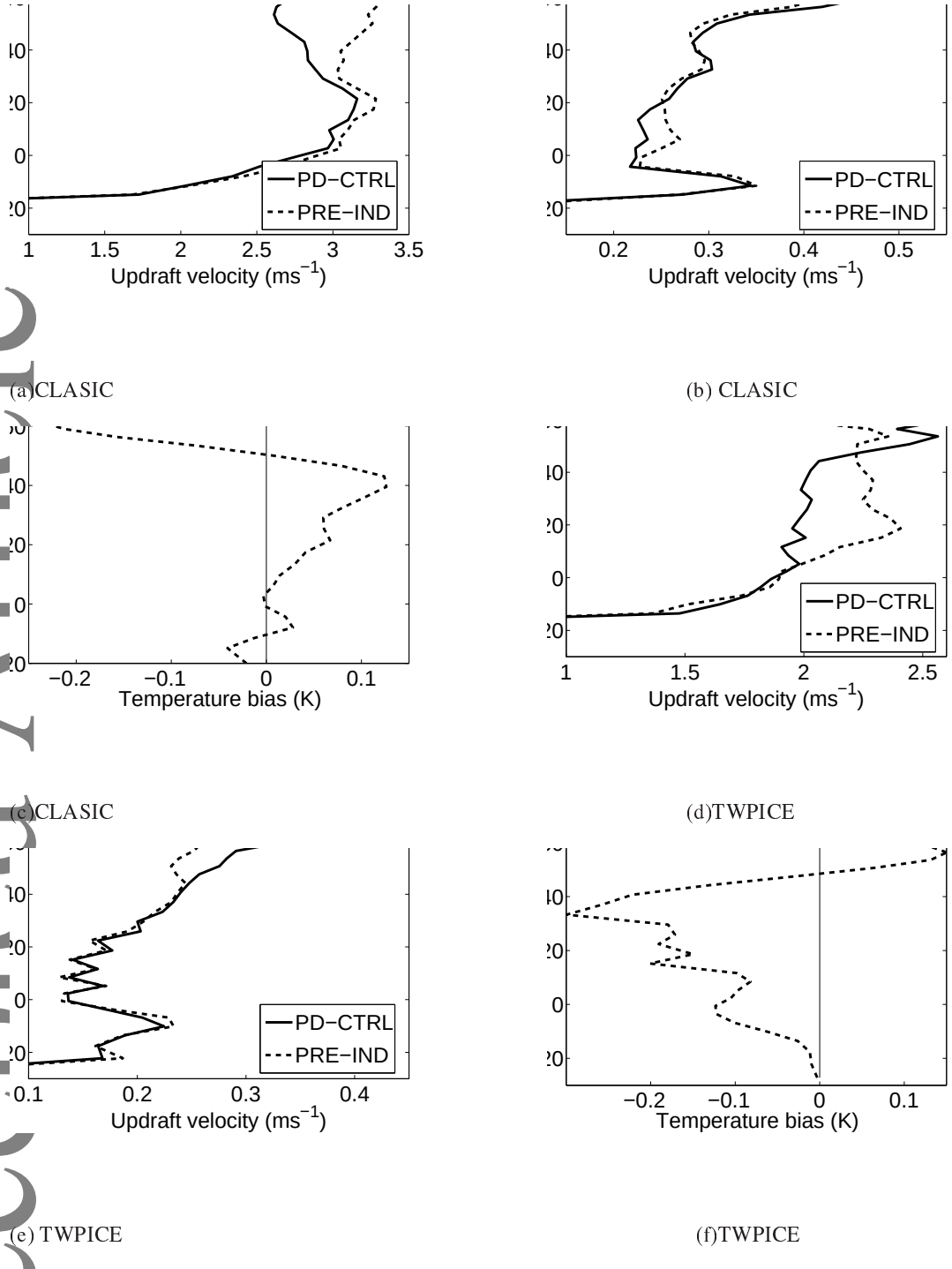

(a)CLASIC (b) CLASIC

(c)CLASIC (d)TWPICE

(e) TWPICE (f)TWPICE

Figure 5. Spatial and temporal averages of updraft speeds in (a) deep convective clouds and (b) in stratiform clouds and (c) is the temperature changes. The upper panel is for the CLASIC case while the lower panel is for the TWPICE case.

both present-day snow and graupel mixing ratios (Figs. 4b and 4c).

The classical glaciation effect enhances ice precipitation as in Connolly et al. (2006). Although there was no specific reference to snow or graupel production in Fan et al. (2010), they reported drying in clear air due to extensive condensation/deposition with increasing IN loading, which implies either more precipitation or merely more cloud or ice content. This was however not the case here and we attributed this predicted reduction to the weakening of updrafts in deep convection convection that we predicted (Figs. 5a).

On the other hand, IWC in TWPICE was marginally insensitive to changes in IN loading, especially below the -60 °C level, although there was a distinct upward shift of the anvil tops clearly exhibited in Fig 4d. This agreed with the patterns predicted for updraft velocities in which the vertical velocities were enhanced in both stratiform and deep convective clouds, especially in the upper-troposphere (see the following section). Both the

unconditional and conditional averages of snow mixing ratios exhibited huge increases in the present day (Fig. 4e) in direct contrast to the mid-latitude continental case where all forms of precipitation were suppressed. This increase in snow mixing ratios was widespread in both cloud types; although the dominant increase was noted in ice-only clouds as opposed to the mixed-phase clouds.

The dominant mechanism by which increased snow mixing ratios were predicted in the solid aerosol pollution scenario was the enhancement of the upper tropospheric number concentrations of ice (Fig. 2d), which also caused substantial warming and strong upper-tropospheric ascent velocities that triggered the upward shift of cloud tops. The upward shifting of the cloud tops also played an important role in the proliferation of snow by deepening the depth of the cloud within which ice crystals could interact and grow to form snow. On the other hand, the mixing ratios of graupel (Fig. 4f) and rain (plot not shown) were hardly changed mainly due to their dependence on the mean diameters of hydrometeors, which remained largely insensitive to solid aerosol pollution.

3.4. Response of Cloud Dynamics to Increased Solid Aerosols

Figs. 5a and 5b show how the glaciation effect affected the dynamics of clouds in CLASIC. Updrafts in deep convective clouds were significantly diminished by as much as 25 %, especially in the present-day upper troposphere, while the effect of IN loading on the intensity of updrafts in stratiform clouds was not substantial, although there is a slight weakening between the 0 °C and the -20 °C levels and a monotonically weak increase above that altitude. Fig. 5c shows the spatially and temporally averaged vertical profile of the temperature bias resulting from increasing IN loading. The profile shows a less than 0.1 °C warming below the homogeneous freezing level. Although this slight warming does not directly explain the general weakening of updrafts predicted over the same range of temperature levels, we attribute the strong upper-tropospheric cooling to the strong reduction in updraft strengths in deep convective clouds. Although this weakening of updrafts is in tandem with many other previous studies such as Fan et al. (2010); Storer and van den Heever (2013) who attributed it to condensate loading, there is no evidence in our case since ice and all other forms of solid precipitation where depleted by IN loading. These results and theirs can however not be compared directly since in Storer and van den Heever (2013)'s case for example, they only varied the CCN and not the IN loadings and also Fan et al. (2010)'s case was a maritime one.

On the other hand, with increased solid aerosol loading, the strength of updrafts increased significantly in the upper troposphere of both stratiform and deep convective clouds in the maritime case (Figs. 5d and 5e). The altitudes within which this strengthening of vertical velocities was exhibited correspond with the altitudes where more ice (Fig. 2d) and more snow (Fig. 4e) were also predicted. This was caused by latent heating released by extra ice and snow during vapour condensational/depositional growth, which is evidenced by the upper tropospheric warming exhibited in Fig. 5f. As a result of the strengthened updrafts, cloud-tops were shifted upwards in the present-present-day. Stronger updrafts have higher momentum to overshoot cloud-tops and detrain moisture and ice in the upper troposphere, which is in keeping with Fan et al. (2010) who found moistening of the upper troposphere when CCN and IN loadings were simultaneously increased. However, the mean velocities of deep convective updrafts below the homogeneous freezing level weakened significantly with IN loading. This corresponded also with a cooling within the same altitude range and since snow production proliferated in the present day, condensate loading may have compounded the weakening of updrafts in the middle troposphere. There was however no sensitivity shown by vertical velocities in the middle tropospheric stratiform clouds.

3.5. Cloud Cover

Generally, the overall horizontal cloud cover averaged over the whole domain increased by about 2 % due to IN pollution in CLASIC; although, different phases of clouds increased with different magnitudes of cloud fractions (Fig. 6a). Mixed-phase clouds exhibited the largest increase in horizontal cloud cover. The main driver of this overall increase in the total cloud fraction was the suppression of precipitation, especially of snow and graupel, which leeds to prolonged cloud lifetimes. The volumetric cloud fraction, Fig. 6c, shows the change in cloudy grid-boxes when the loading of solid aerosols was increased. The values of the change

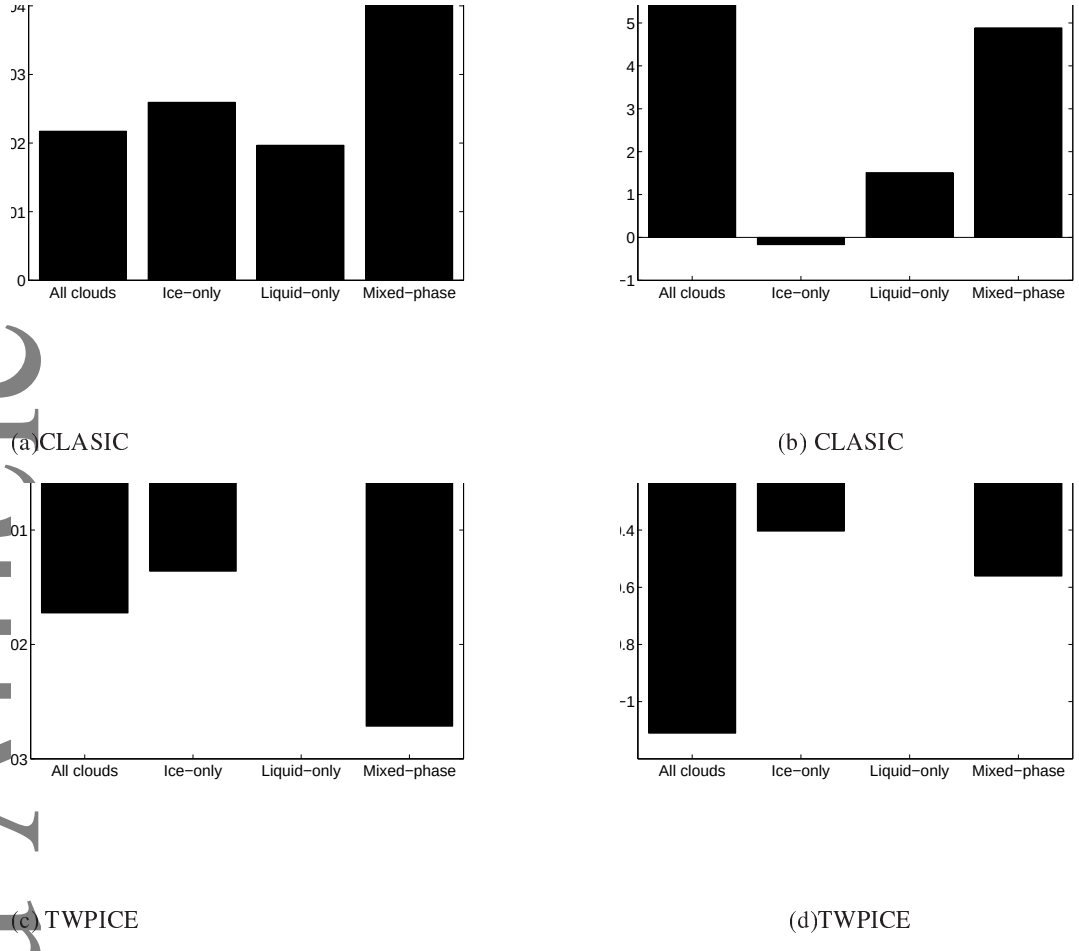

Figure 6. Changes in horizontal cloud fractions and volumetric cloud fractions are presented in (a) and (b), respectively. The upper panel is for the CLASIC case while the lower panel is for the TWPICE case. The volumetric cloud fraction represents the number of cloudy grid-boxes.

in volumetric cloud fraction are very small because the total number of grid boxes in the 2-D domain is over 4000 and all these are written out every 5 minutes for three weeks, hence, a fraction change in the number of cloudy grid boxes appears small, but it is meaningful. The volumetric cloud fraction also exhibited similar trends of increasing cloud cover in the present day. It is noteworthy that the volumetric cloud fraction of ice-only clouds showed a significant weakening in the present-day simulation relative to the preindustrial solid-aerosol run. This decrease is mainly attributed to the predicted decrease in upper tropospheric ice water content (IWC) 4a. This finding of an increase in horizontal cloud fractions exhibited by all clouds in this mid-latitude continental case is contrary to the widely accepted understanding that, the glaciation indirect effect favours the ice crystal process, which in principle, should diminish the liquid-phase components of the clouds and increase precipitation via the ice-phase.

Overall, there was a net reduction in cloud cover due to solid aerosol pollution in TWPICE (Fig. 6c). The mixed-phase clouds showed an increase in contrast with the continental case where an increase in solid aerosol number concentration resulted in an increase in the cloud fraction. The main cause for this reduction in cloud cover is the predicted increase in snow production (Fig. 4e). Precipitation production via the ice-phase is more efficient than via the warm phase; hence, the cloud lifetime diminishes quickly under such a scenario. The volumetric cloud fraction was also severely depleted indicating that the number of cloudy grid-points was reduced in the present day simulation. Overall, a net reduction of about 2% in cloud fraction was caused by increased solid aerosol pollution.

3.6. Response of Cloud Optical Properties to Increased Solid Aerosols

The intrinsic and domain-wide changes in the optical thicknesses (τ_i) between the pre-industrial and the present-day scenarios shown in Figs. 7a and 7b, respectively for the CLASIC case show very small changes overall. In the present day however, the intrinsic optical thickness of all clouds showed a slight reduction.

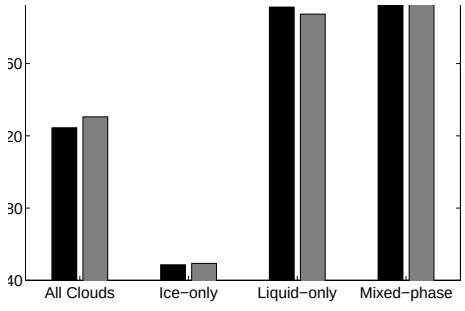

(a) CLASIC

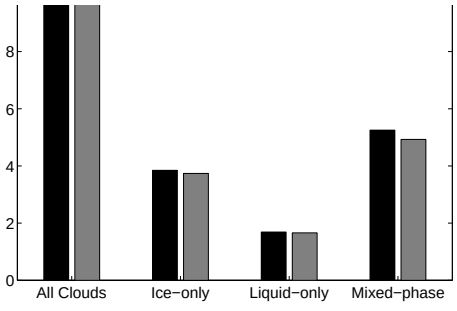

(b) CLASIC

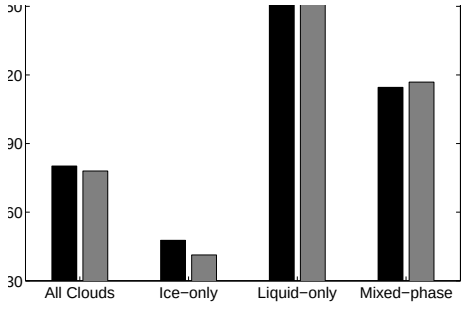

(c) TWPICE

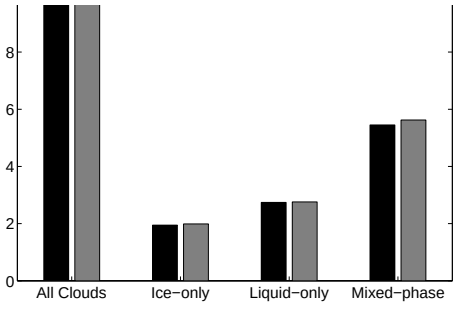

(d) TWPICE

Figure 7. Changes in horizontal the intrinsic and unconditionally averaged optical thicknesses of clouds are presented in (a) and (b), respectively. The upper panel is for the CLASIC case while the lower panel is for the TWPICE case.

While there was no significant change evident in the τ_i of ice-only and mixed phase clouds, there was however a slight increase in τ_i for the liquid-only clouds. This reduction in the present-day intrinsic optical thickness of all clouds is reminiscent of the reduction in the upper-tropospheric ice water content (4a). As for the unconditional averages, the overall optical thicknesses of all clouds was higher in the present-day run, mainly because both the horizontal and volumetric cloud fractions increased with increased solid aerosols. In other words, clouds became more extensive but optically thinner due to solid aerosol pollution.

On the other hand, in TWPICE, despite the significant increases in snow production when solid aerosol loading was increased, the overall intrinsic optical thickness of all clouds was hardly sensitive, although a very weak increase was seen. Ice-only clouds showed a slight increase, while the mixed-phase phase and water-only clouds exhibited a reduction in present day τ_i, with water-only clouds showing the largest drop. Considering that more snow was produced in ice-only clouds and the IWC was actually depleted in the present-day run, this increase of the optical thickness in ice-only clouds can only be attributed to a predicted present-day increase in the depth of clouds and not to the intensification of the water contents. Other types of clouds became slightly optically thinner largely because of the depletion of the volumetric cloud fractions caused by the increase in snow. The unconditionally averaged optical thicknesses of the clouds were decreased in the present-day simulation mainly because the horizontal cloud fractions decreased in the present-day (Fig. 7d).

4. Results for Response of Cloud Radiative Properties to Increased Solid Aerosols

4.1. Responses from the Continental Case (CLASIC)

Of the -1.96 Wm^{-2} radiative forcing from all clouds, the contribution from water-only clouds, -1.22 $\pm$ 0.18 Wm^{-2}, was higher than the contribution from glaciated clouds, -0.74 $\pm$ 0.11 Wm^{-2}, both were resolved from Test C. The indirect effect of water-only clouds was stronger than that of ice-only clouds despite the fact that Fig. 6a exhibits an increase in the coverage of

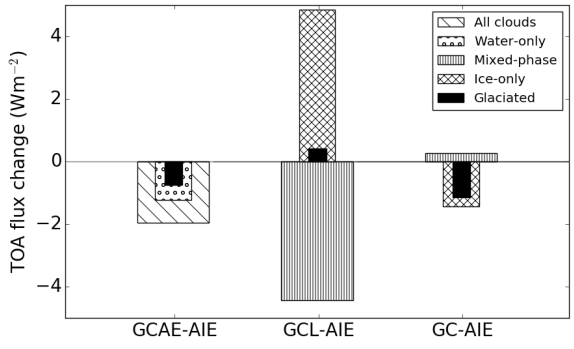

Figure 8. The glaciation aerosol indirect effect, arising from increasing solid aerosol concentrations in CLASIC. Meanings of abbreviations: GC-AIE = Glaciated Clouds AIE, GCL-AIE = Glaciated Clouds Lifetime AIE, GCAE-AIE = Glaciated Clouds Albedo-Emissivity AIE.

glaciated clouds that is higher than that of the liquid-only clouds. The increase in the glaciated cloud fraction being relatively higher than that of liquid-only clouds. On the other hand, mixed-phase clouds exhibited a much higher change in cloud fractions, hence it is not intuitive to derive a conclusion from this relationship between radiative flux changes and domain-wide changes in cloud fractions. However, from Fig. 6b, it is shown that there was a slight negative change in the volumetric cloud coverage of ice-only clouds. This weak response by ice-only volumetric cloud cover explains the smaller contribution of glaciated clouds to the net radiative flux change of all clouds relative to water-only clouds. This is also corroborated by Fig. 7a, which shows that only liquid-only clouds had the intrinsic optical thickness that increased in the present-day, while for the domain-wide optical thickness (Fig. 7b), only mixed-phase clouds exhibited a significant increase in the optical thickness.

From Fig. 8, it is shown that the net glaciated clouds lifetime indirect effect (GCL-AIE), estimated using the Test C is actually positive, i.e. 0.41 ± 0.06 Wm^{-2} signifying a warming effect on the climate system. This is despite the net increase in the domain-wide average of the cloud fraction of ice-only and mixed-phase clouds from solid aerosol pollution. This positive radiative forcing is attributed to the reduction in the intrinsic optical thicknesses of ice-only clouds. The limited drop in the volumetric cloud cover of ice-only clouds also indicates that they became optically thinner in the present-day, making them reflect back to space less incoming shortwave radiation, which explains also why the component of the glaciated lifetime indirect effect from ice-only clouds was strongly positive (4.85 ± 1.35 Wm^{-2}). The reduction in the optical thickness of ice-only clouds was also corroborated by the upper troposphere reduction in ice mixing ratios (Fig. 4a). On the other hand, the component of the glaciated cloud lifetime indirect effect from mixed-phase clouds is strongly negative (-4.44 ± 1.33 Wm^{-2}) mainly because its optical thickness increased with increasing solid aerosols.

Although there is no significant change in the mean sizes of cloud particles shown, there was a weak bias towards smaller sizes in the present-day and this might have had a bias towards increasing the reflectance of cloud particles, hence, a net cooling effect from the albedo-emissivity effect of -1.15 ± 0.11 Wm^{-2} was predicted using the Test B.

4.2. *Responses from the Maritime Case (TWPICE)*

The classical glaciation effect, such as the one found by Storelvmo et al. (2011) in their global modelling study of IN effects on mixed-phase clouds was exhibited in this maritime case (Fig. 9). A positive radiative forcing of about 1 Wm^{-2} was predicted in the TWPICE case, implying a warming effect. This positive forcing was primarily caused by the distinct drop in cloud cover for both the domain-wide horizontal and volumetric averages (Figs 6c and 6d, respectively) owing to a strong increase in present-day snow production. The domain-wide optical thickness, Fig. 7d, shows that present-day clouds were generally optically thinner, hence they allow more solar radiation into the atmosphere leading to this warming effect. The primary cause for these two responses was the predicted increase in snow production, which was more distinct in ice-only clouds. As a result, the contributions to this warming effect by the glaciation indirect effect were dominated by glaciated clouds, which exhibited a strongly positive radiative forcing of about 4.74 ± 1.66 Wm^{-2}, while the water-only clouds actually had a negative radiative flux change at the TOA (-3.72 ± 1.3 Wm^{-2}). This is because water-only clouds were hardly sensitive to the solid aerosol increase in their domain-wide cloud coverage (Fig. 6c), even their volumetric cloud fractions exhibited the least change among all other cloud types. This is not surprising because solid aerosols are not the dominant source of cloud droplets in the model or in the atmosphere.

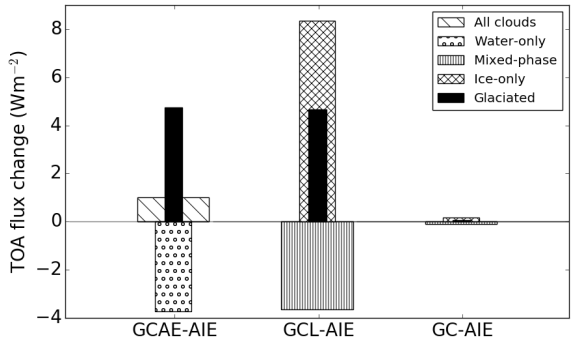

Figure 9. The glaciation aerosol indirect effect, arising from increasing solid aerosol concentrations in TWPICE. Meanings of abbreviations: GC-AIE = Glaciated Clouds AIE, GCL-AIE = Glaciated Clouds Lifetime AIE, GCAE-AIE = Glaciated Clouds Albedo-Emissivity AIE.

Of the net glaciation effect of 4.74 ± 1.66 Wm^{-2} from the glaciated clouds, the largest contribution to this warming effect was from ice-only clouds, which contributed a forcing of about 8.51 ± 2.98 Wm^{-2}. The mixed-phase clouds' contribution to this forcing was actually a negative radiative forcing of about -3.77 ± 1.3 Wm^{-2}. This is because the largest notable increase in snow mixing ratio was predicted in ice-only clouds, while no substantial changes were simulated in mixed-phase clouds.

Finally, because the mean sizes of cloud particles were largely unchanged for both cloud droplets and ice crystals due to the increase in solid aerosols, the resultant albedo-emissivity indirect effect was insignificant in all cloud types, implying that the warm-cloud albedo indirect effect signature in maritime clouds due to solid aerosol pollution is quite faint. This is mainly because, the background solid aerosol concentrations of marine clouds are relatively low compared to their continental counterparts, and also the change in the solid aerosol loading in this already clean maritime air caused by anthropogenic activities is very low when compared to the continental air. Hence, with good confidence, we can conclude that the glaciation effect is more distinct in clean maritime clouds than in more polluted continental clouds, while the warm-cloud albedo indirect effect is more pronounced in continental clouds.

5. Conclusion

This investigation examined the microphysical and dynamical mechanisms by which solid aerosols affect the radiative properties of clouds. The simulations were conducted using a state-of-the-art hybrid bin model coupled to the Weather Research and Forecasting (WRF) model. The scheme treats five species of hydrometeors, i.e. cloud, ice, rain, snow and graupel (TWPICE). Two cases of deep convection were chosen for this study, the first one was a continental mid-latide case (CLASIC), while the other one was a tropical maritime case. The main difference between the two cases was in their background aerosol burdens, the continental case was highly polluted, while the maritime case was quite pristine.

In the mid-latitude continental case (CLASIC), the key microphysical and dynamical mechanisms identified were as follows. Firstly, the increase in solid aerosols caused the cloud droplet number concentrations to rise slightly, especially in sub-zero temperatures owing to the internal mixing and wettability assumed for solid aerosol which allows them to act as extra CCN, while the ice crystal number concentrations were essentially insensitive to aerosol changes mainly because primary heterogeneous nucleation of ice crystals by solid aerosol is not the dominant source of ice concentrations. However, there was significant suppression of precipitation production in the present-day attributed to a significant reduction in the strength of deep convective updraft speeds. A corresponding reduction in present-day upper tropospheric ice water contents was also predicted. The weakening of updraft velocities in convective clouds by as much as 25 % especially in the upper troposphere was attributed mainly to the predicted strong present-day upper-tropospheric cooling and partly to condensate loading in the middle troposphere. Consequently, weaker updrafts reduced upper tropospheric IWC and suppressed precipitation production and anvil outflow while causing increased cloud cover and prolonged cloud lifetime - all of which increase the reflectance of the cloud. As such, the simulations showed that solid aerosols had a net cooling effect (-1.96 ± 0.29 Wm^{-2}) in the continental case (CLASIC).

As for the maritime case, the number concentration of cloud droplets was hardly sensitive to increased solid aerosol due to the low fractional contribution of solid aerosol to primary cloud activation, but ice crystal number concentrations showed a substantial increase particularly in the upper troposphere. This increase was driven primarily by an increase in the homogeneous freezing of cloud droplets facilitated by strong vertical velocities predicted aloft and heterogeneous nucleation of ice by extra

IN. The well pronounced strengthening of updrafts in the upper-troposphere in both deep-convective and stratiform clouds resulted from the latent heating caused the proliferation of ice crystals. These strong updrafts also prompted a distinct upward shift of cloud tops. The increase in ice crystal concentrations promoted precipitation production especially of snow via the ice phase process in regions of stratiform cloud formed by convective outflow, thereby depleting the cloud cover and optical thickness of cloud particles. As a result of the depleted cloud cover and optical thickness, greater radiative fluxes were transmitted through the atmosphere, thereby causing a net warming effect of 1 Wm^{-2} for this maritime case.

In our previous study (Kudzotsa et al. 2016a), we investigated how changes in solute aerosols affect the riming, aggregation and coalescence processes in clouds. We discovered that these processes are weakened by more solute aerosols in such a way that they cause a cooling effect on the climate. In this present study, the same tests were conducted to investigate the role of solid aerosol on these processes. The effect of solid aerosols on these process was insignificant. This was attributed to the fact that the increases and the background amounts of solid aerosols were much lower in comparison to solute aerosols.

In conclusion, it has been noted that clouds responded differently, both microphysically and dynamically to increasing solid aerosol loading between the continental and the maritime atmospheres. The glaciation indirect effect was more pronounced in the maritime case, where a strong warming effect was predicted than in the continental case where a cooling effect was noted. Although, the thermodynamic environment has been shown to also be different between the two cases (Fig. 1), this finding is in tandem with other previous studies e.g., Andreae et al. (2007) who discovered that for a given cloud type, with the same thermodynamic environment, the aerosol indirect effects are larger in cleaner clouds than in polluted clouds. In other words, maritime clouds would be expected to be more sensitive to aerosol changes than continental clouds.

References

Allen, G., et al., 2008: Aerosol and trace-gas measurements in the darwin area during the wet season. *Journal of Geophysical Research*, **113**, D06 306, doi: 10.1029/2007JD008706.

Andreae, M. O. et al., 2007: Aerosols before pollution. *Science(Washington)*, **315 (5808)**, 50–51.

Boucher, O. and D. Randall, 2013: Climate change 2013: The physical science basis. contribution of working group i to the fifth assessment report of the intergovernmental panel on climate change, (ipcc). *Cambridge University Press, Cambridge, United Kingdom and New York, NY, USA.*, **5th**.

Carrió, G., S. van den Heever, and W. Cotton, 2007: Impacts of nucleating aerosol on anvil-cirrus clouds: A modeling study. *Atmospheric research*, **84 (2)**, 111–131.

Carslaw, K., et al., 2013: Large contribution of natural aerosols to uncertainty in indirect forcing. *Nature*, **503 (7474)**, 67.

Charlson, R., S. E. Schwartz, J. Hales, R. Cess, J. J. Coakley, H. JE., and H. DJ., 1992: Climate forcing by anthropogenic aerosols. *Science*, **255 (5043)**, 423–30.

Connolly, P. J., T. W. Choularton, M. W. Gallagher, K. N. Bower, M. J. Flynn, and J. A. Whiteway, 2006: Cloud-resolving simulations of intense tropical hector thunderstorms: Implications for aerosol-cloud interactions. *Q.J.R. Meteorol. Soc.*, **132**, 3079–3106, doi:10.1256/qj.05.86.

Costantino, L. and F. M. Breon, 2013: Aerosol indirect effect on warm clouds over south-east atlantic, from co-located modis and calipso observations. *Atmospheric Chemistry and Physics*, **13**, 69–88.

Cui, Z., K. S. Carslaw, Y. Yin, and S. Davies, 2006: A numerical study of aerosol effects on the dynamics and microphysics of a deep convective cloud in a continental environment. *J. Geophys. Res.*, **111 (D05)**, D05 201.

Cziczo, D. J., D. M. Murphy, P. K. Hudson, and D. S. Thomson, 2004: Single particle measurements of the chemical composition of cirrus ice residue during crystal-face. *J. Geophys. Res*, **109**, D04 201.

DeMott, P. J., et al., 2010: Predicting global atmospheric ice nuclei distributions and their impacts on climate. *Proceedings of the National Academy of Sciences*, **107 (25)**, 11 217–11 222.

DeMott, P. J., et al., 2011: Resurgence in ice nuclei measurement research. *Bull. Amer. Meteor. Soc*, **92**, 1623–1635.

Diehl, K., S. Matthias-Maser, R. Jaenicke, and S. Mitra, 2002: The ice nucleating ability of pollen:: Part ii. laboratory studies in immersion and contact freezing modes. *Atmospheric research*, **61 (2)**, 125–133.

Diehl, K., C. Quick, S. Matthias-Maser, S. Mitra, and R. Jaenicke, 2001: The ice nucleating ability of pollen: Part i: Laboratory studies in deposition and condensation freezing modes. *Atmospheric Research*, **58 (2)**, 75–87.

Dymarska, M., B. J. Murray, L. Sun, M. L. Eastwood, D. A. Knopf, and A. K. Bertram, 2006: Deposition ice nucleation on soot at temperatures relevant for the lower troposphere. *Journal of Geophysical Research: Atmospheres (1984–2012)*, **111 (D4)**.

Ekman, A., A. Engström, and C. Wang, 2007: The effect of aerosol composition and concentration on the development and anvil properties of a continental deep convective cloud. *Quarterly Journal of the Royal Meteorological Society*, **133 (627)**, 1439–1452.

Fan, J., J. M. Comstock, and M. Ovchinnikov, 2010: The cloud condensation nuclei and ice nuclei effects on tropical anvil characteristics and water vapor of the tropical tropopause layer. *Environmental Research Letters*, **5 (4)**, 044 005.

Fan, J., D. Rosenfeld., L. Yanni Ding, R. Leung., and Z. Li, 2012: Potential aerosol indirect effects on atmospheric circulation and radiative forcing through deep convection. *Geophysical Research Letters*, **39 (9)**, L09 806.

Ferrier, B. S., 1994: A double-moment multiple-phase four-class bulk ice scheme. part i: Description. *J. Atmos. Sci.*, **51**, 249–280.

Freidenreich, S. M. and V. Ramaswamy, 1999: A new multiple-band solar radiative parameterization for general circulation models. *J. Geophys. Res*, **104 (D24)**, 31 389–31 409.

Gettelman, A., X. Liu, D. Barahona, D. Lohmann, and C. Chen, 2012: Climate impacts of ice nucleation. *Journal of Geophysical Research: Atmospheres*, **117 (D20)**, D20 201.

Haywood, J. and O. Boucher, 2000: Estimates of the direct and indirect radiative forcing due to tropospheric aerosols: A review. *Reviews of Geophysics*, **38 (4)**, 513–543.

Hoeve, T. J. E., L. A. Remer, and M. Z. Jacobson, 2011: Microphysical and radiative effects of aerosols on warm clouds during the amazon biomass burning season as observed by modis: impacts of water vapor and land cover. *Atmos. Chem. Phys.*, **11**, 3021–3036.

Hoppel, W. A., G. M. Frick, and J. W. Fitzgerald, 2002: Surface source function for sea-salt aerosol and aerosol dry deposition to the ocean surface. *Journal of Geophysical Research: Atmospheres*, **107 (D19)**, AAC 7–1–AAC 7–17, doi:10.1029/2001JD002014, URL `http://dx.doi.org/10.1029/2001JD002014`.

Jaenicke, R., 2005: Abundance of cellular material and proteins in the atmosphere. *Science*, **308 (5718)**, 73–73.

Khain, A., D. Rosenfeld, and A. Pokrovsky, 2001: Simulating convective clouds with sustained supercooled liquid water down to- 37.5 c using a spectral microphysics model. *Geophysical Research Letters*, **28 (20)**, 3887–3890.

Khain, A., D. Rosenfeld, and A. Pokrovsky, 2005: Aerosol impact on the dynamics and microphysics of deep convective clouds. *Quarterly Journal of the Royal Meteorological Society*, **131 (611)**, 2639–2663.

Khairoutdinov, M. and Y. Kogan, 2000: A new cloud physics parameterization in a large-eddy simulation model of marine stratocumulus. *American Meteorological Society*, **128**, 229–243.

Kudzotsa, I., 2013: Mechanisms of aerosol indirect effects on glaciated clouds simulated numerically. Ph.D. thesis, University of Leeds, UK.

Kudzotsa, I., V. J. P. Phillips, and S. Dobbie, 2016a: Aerosol indirect effects on glaciated clouds. part ii: Sensitivity tests. *QJRMS*.

Kudzotsa, I., et al., 2016b: Aerosol indirect effects on glaciated clouds. part i: Model description. *QJRMS*.

Lee, S. S., L. J. Donner, and V. Phillips, 2009: Sensitivity of aerosol and cloud effects on radiation to cloud types: comparison between deep convective clouds and warm stratiform clouds over one-day period. *Atmos Chem Phys*, **9**, 2555–2575.

Lee, S.-S., F. Graham, and P. Y. Chuang, 2012: Effect of aerosol on cloud-environment interactions in trade cumulus. *J. Atmos. Sci*, **69**, 3607–3632.

Liu, C., 2011: Rainfall contributions from precipitation systems with different sizes, convective intensities, and durations over the tropics and subtropics. *Journal of Hydrometeorology*, **12 (3)**, 394–412.

Lohmann, U., 2002a: A glaciation indirect aerosol effect caused by soot aerosols. *Geophysical Research Letters*, **29**, doi:10.1029/2001GL014357.

Lohmann, U. and J. Feichter, 2005: Global indirect aerosol effects: a review. *Atmospheric Chemistry and Physics*, **5 (3)**, 715–737, doi:10.5194/acp-5-715-2005, URL `http://www.atmos-chem-phys.net/5/715/2005/`.

Martin, G., D. Johnson, and A. Spice, 1994: The measurement and parameterization of effective radius of droplets in warm stratocumulus clouds. *Journal of the Atmospheric Sciences*, **51 (13)**, 1823–1842.

May, P. T., J. H. Mather, V. Geraint, B. Keith N., J. Christian, M. Greg M., and M. Gerald G., 2008: The tropical warm pool international cloud experiment. *American Meteorological Society*, **89**, 629–645, doi:http://dx.doi.org/10.1175/BAMS-89-5-629.

Meyers, M. P., P. J. DeMott, and W. R. Cotton, 1992: New primary ice-nucleation parameterizations in an explicit cloud model. *Journal of Applied Meteorology*, **31 (7)**, 708–721.

Michalakes, J., J. Dudhia, D. Gill, T. Henderson, J. Klemp, W. Skamarock, and W. Wang, 2005: The weather research and forecast model: software architecture and performance. *Use of High Performance Computing in Meteorology*, World Scientific, 156–168.

Miller, M. A., 2007: Sgp cloud and land surface interaction campaign (clasic): Science and implementation plan. *DOE/SC-ARM-0703*.

Ming, Y., V. Ramaswamy, L. J. Donner, and V. T. J. Phillips, 2006: A new parameterization of cloud droplet activation applicable to general circulation models. *Journal of the atmospheric sciences*, **63**, 1348–1356.

Murray, B. J., et al., 2010: Heterogeneous nucleation of ice particles on glassy aerosols under cirrus conditions. *Nature Geosci*, **3**, 233–237, doi:10.1038/ngeo817.

Petters, M. D. and S. M. Kreidenweis, 2007: A single parameter representation of hygroscopic growth and cloud condensation nucleus activity. *Atmospheric Chemistry and Physics*, **7 (8)**, 1961–1971, doi:10.5194/acp-7-1961-2007, URL `http://www.atmos-chem-phys.net/7/1961/2007/`.

Phillips, V. T., et al., 2017: Ice multiplication by breakup in ice–ice collisions. part ii: Numerical simulations. *Journal of the Atmospheric Sciences*, **74 (9)**, 2789–2811.

Phillips, V. T. J., C. Andronache, B. C. E. Morris, D. C. Sands, A. Bansemer, A. Lauer, C. McNaughton, and C. Seman, 2009: Potential impacts from biological aerosols on ensembles of continental clouds simulated numerically. *Biogeosciences*, **6**, 987–1014.

Phillips, V. T. J., P. J. DeMott, and C. Andronache, 2008: An empirical parameterization of heterogeneous ice nucleation for multiple chemical species of aerosol. *Journal of the atmospheric sciences*, **65**, 2757–2783, doi:10.1175/2007JAS2546.1.

Phillips, V. T. J., P. J. Demott, C. Andronache, K. A. Pratti, and C. Twohy, 2013: Improvements to an empirical parameterization of heterogeneous ice nucleation and its comparison with observations. *J. Atmos. Sci.*, **70**, 378–409.

Phillips, V. T. J., L. J. Donner, and S. T. Garner, 2007: Nucleation processes in deep convection simulated by a cloud-system-resolving model with double-moment bulk microphysics. *Journal of the Atmospheric Sciences*, **64**, 738–761, doi:http://dx.doi.org/10.1175/JAS3869.1.

Platt, C., 1973: Lidar and radiometric observations of cirrus clouds. *Journal of the atmospheric sciences*, **30 (6)**, 1191–1204.

Prabhakara, C., D. Kratz, J.-M. Yoo, G. Dalu, and A. Vernekar, 1993: Optically thin cirrus clouds: Radiative impact on the warm pool. *Journal of Quantitative Spectroscopy and Radiative Transfer*, **49 (5)**, 467–483.

Rap, A., C. E. Scott, D. V. Spracklen, N. Bellouin, P. M. Forster, K. S. Carslaw, A. Schmidt, and G. Mann, 2013: Natural aerosol direct and indirect radiative effects. *Geophysical Research Letters*, **40 (12)**, 3297–3301.

Rogers, R. R. and M. K. Yau, 1991: *A short course in cloud physics*. 3d ed., Perganom.

Romakkaniemi, S., A. Jaatinen, A. Laaksonen, A. Nenes, and T. Raatikainen, 2014: Ammonium nitrate evaporation and nitric acid condensation in dmt ccn counters. *Atmospheric Measurement Techniques*, **7 (5)**, 1377–1384.

Saleeby, S., S. Heever, P. Marinescu, S. Kreidenweis, and P. DeMott, 2016: Aerosol effects on the anvil characteristics of mesoscale convective systems. *Journal of Geophysical Research: Atmospheres*, **121 (18)**.

Sheffield, A. M., S. M. Saleeby, and S. C. Heever, 2015: Aerosol-induced mechanisms for cumulus congestus growth. *JGR: Atmospheres*, **120 (17)**, 8941–8952.

Shupe, M. D., et al., 2008: A focus on mixed-phase clouds: The status of ground-based observational methods. *Bulletin of the American Meteorological Society*, **89 (10)**, 1549–1562.

Solomon, S., D. Qin, M. Manning, Z. Chen, M. Marquis, K. Averyt, M.Tignor, and H. M. (eds.), 2007: Climate change 2007: The physical science basis. contribution of working group i to the fourth assessment report of the intergovernmental panel on climate change, (ipcc). *Cambridge University Press, Cambridge, United Kingdom and New York, NY, USA.*, **4th**.

Storelvmo, T., C. Hoose, and P. Eriksson, 2011: Global modeling of mixed-phase clouds: The albedo and lifetime effects of aerosols. *Journal of Geophysical Research: Atmospheres*, **116 (D5)**.

Storer, R. L. and S. C. Van den Heever, 2013: Microphysical processes evident in aerosol forcing of tropical deep convective clouds. *Journal of the Atmospheric Sciences*, **70 (2)**, 430–446.

Storer, R. L. and S. C. van den Heever, 2013: Microphysical processes evident in aerosol forcing of tropical deep convective clouds. *J. Atmos. Sci*, **70 (2)**, 430–446.

Swann, H., 1998: Sensitivity to the representation of precipitating ice in crm simulations of deep convection. *Atmospheric Research*, **47-48**, 415–435.

Takemura, T., 2012: Distributions and climate effects of atmospheric aerosols from the preindustrial era to 2100 along representative concentration pathways (rcps) simulated using the global aerosol model sprintars. *Atmos. Chem. Phys.*, **12**, 11 555–11 572.

Tao, W.-K., X. Li, A. Khain, T. Matsui, S. Lang, and J. Simpson, 2007: Role of atmospheric aerosol concentration on deep convective precipitation: Cloud-resolving model simulations. *JGR: Atmospheres*, **112 (D24)**.

Tompkins, A., 2000: The impact of dimensionality on long-term cloud-resolving model simulations. *Monthly Weather Review*, **128 (5)**.

Twohy, C. H., et al., 2009: Saharan dust particles nucleate droplets in eastern atlantic clouds. *Geophysical Research Letters*, **36 (1)**.

Twomey, S., 1974: Pollution and the planetary albedo. *Atmospheric Environment*, **8**, 1251–1256.

Twomey, S. A., 1977: The influence of pollution on the shortwave albedo of clouds. *Journal of the Atmospheric Sciences*, **34 (7)**, 1149–1152.

Van den Heever, S. C., G. G. Carrió, W. R. Cotton, P. J. DeMott, and A. J. Prenni, 2006: Impacts of nucleating aerosol on florida storms. part i: Mesoscale simulations. *Journal of the atmospheric sciences*, **63 (7)**, 1752–1775.

Verlinde, J., et al., 2007: The mixed-phase arctic cloud experiment. *Bulletin of the American Meteorological Society*, **88 (2)**, 205–222.